

Indigo chromophores: structure and dynamics.

V. V. Volkov,^a R. Chelli,^b R. Righini,^c C. C. Perry^a

^a*Interdisciplinary Biomedical Research Centre, School of Science and Technology, Nottingham Trent University, Clifton Lane, Nottingham NG11 8NS, United Kingdom*

^b*Dipartimento di Chimica, Università di Firenze, Via della Lastruccia 3, I-50019 Sesto Fiorentino, Italy*

^c*European Laboratory for Nonlinear Spectroscopy (LENs), Università di Firenze, Via Nello Carrara 1, I-50019 Sesto Fiorentino, Italy*

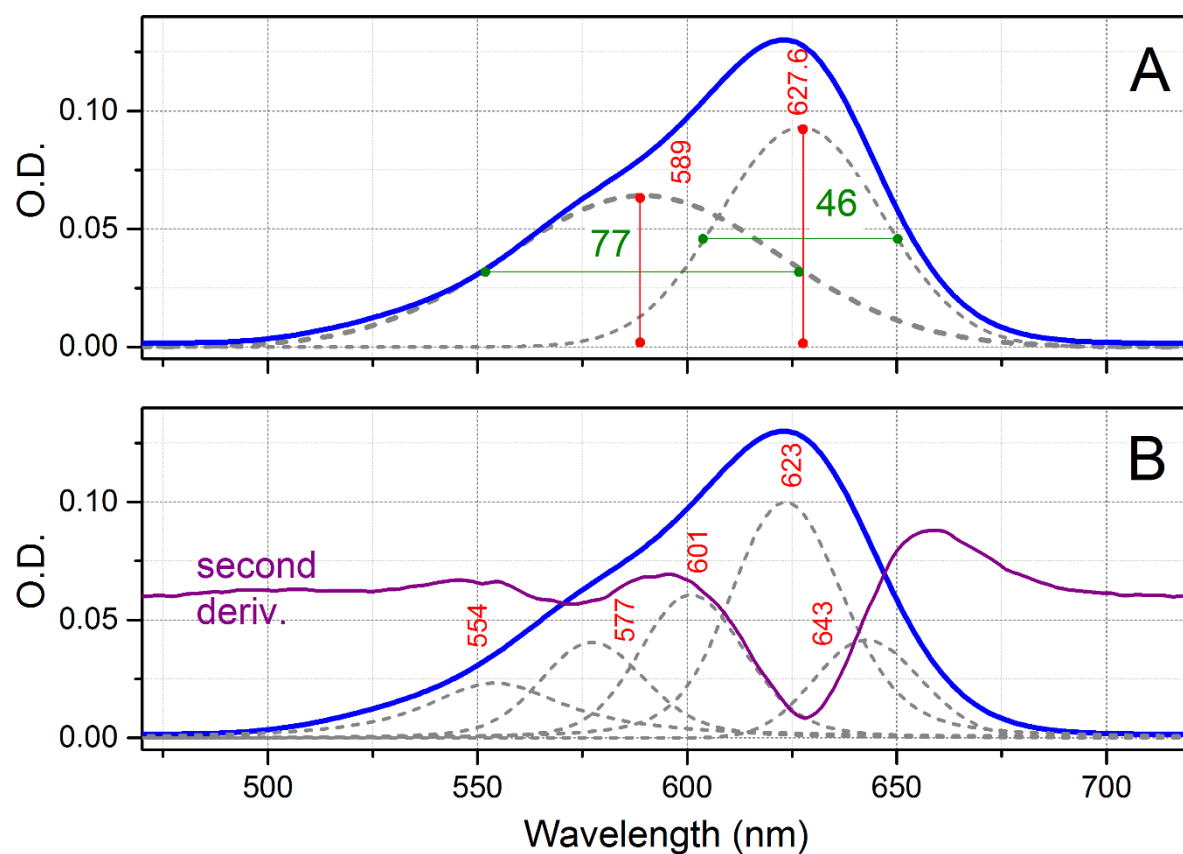


Fig. S1. The simplest (panel A) and the second-derivative assisted (panel B) fits of the optical absorption of indigo carmine in DMSO.

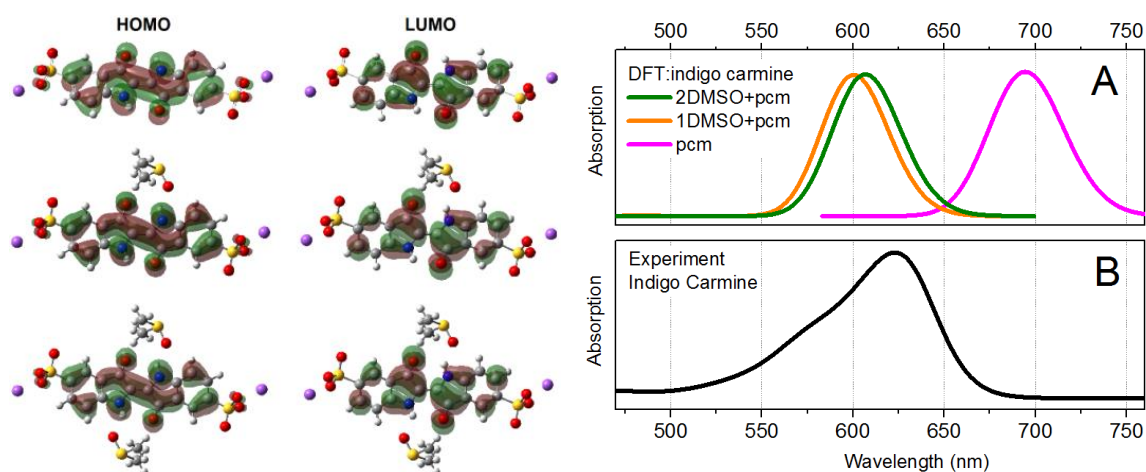


Fig. S2. Chemical structures of *trans* indigo carmine alone (environment is addressed with polarizable continuum model, PCM), with one DMSO molecule hydrogen bonded to a NH moiety (under PCM) and with two DMSO molecules hydrogen bonded to NH moieties together (under PCM) with the molecular orbitals involved in optical excitation in the visible spectral range calculated by TD-DFT. Panel A: spectra calculated by TD-DFT for the model systems shown on the left. Panel B: UV-VIS Optical Absorption properties of indigo carmine solution in deuterated DMSO.

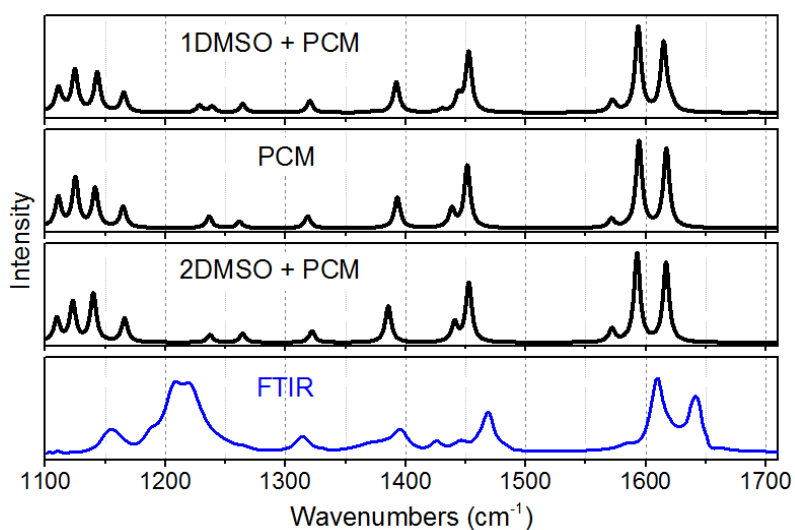


Fig. S3. Three top panels: Mid-IR spectral responses anticipated with DFT for *trans* indigo carmine alone (environment is addressed with PCM), with one DMSO molecule hydrogen bonded to a NH moiety (under PCM) and with two DMSO molecules hydrogen bonded to NH moieties as described in Fig. S2 (under PCM). Bottom panel: FTIR spectrum of indigo carmine solution in deuterated DMSO.

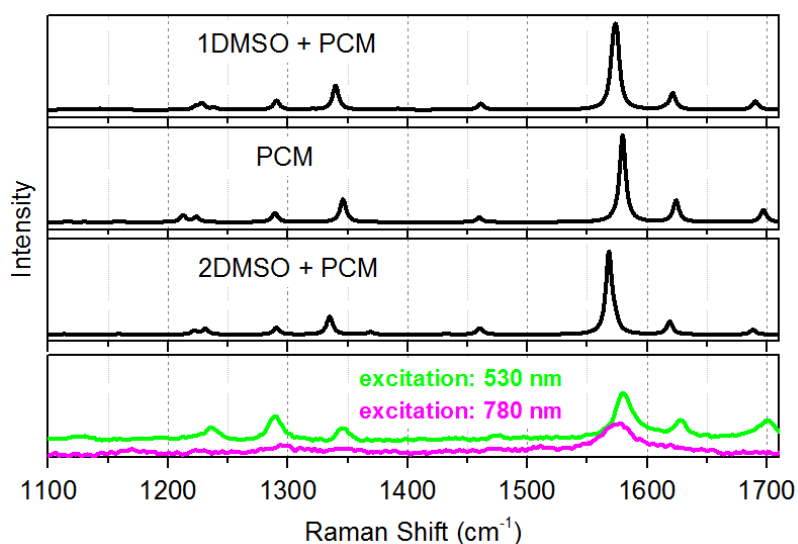


Fig. S4. Three top panels: Mid-IR Raman spectral responses anticipated with DFT for *trans* indigo carmine alone (environment is addressed with PCM), with one DMSO molecule hydrogen bonded to a NH moiety (under PCM) and with two DMSO molecules hydrogen bonded to NH moieties as described in Fig. S2 (under PCM). Bottom panel: Resonant Raman spectrum of indigo carmine solution in deuterated DMSO detected under excitation at 530 nm; and Nonresonant Raman spectrum of solid indigo carmine solution detected under excitation at 780 nm.

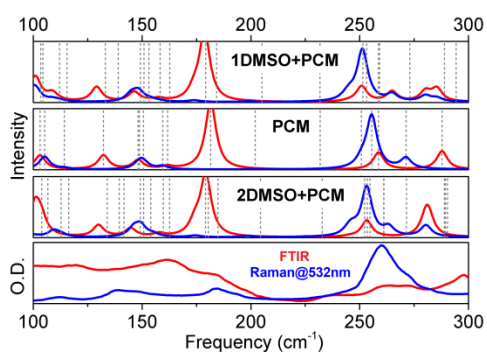


Fig. S5. Three top panels: Far infrared (red) and Raman (blue) spectral responses anticipated with DFT for *trans* indigo carmine alone (environment is addressed with PCM), with one DMSO molecule hydrogen bonded to a NH moiety (under PCM) and with two DMSO molecules hydrogen bonded to NH moieties as described in Fig. S2 (under PCM); grey dashed lines indicate the calculated resonances. Bottom panel: FTIR spectrum of solid indigo carmine (red line), and resonant Raman spectrum (blue line) of indigo carmine solution in deuterated DMSO detected using excitations at 532 nm.

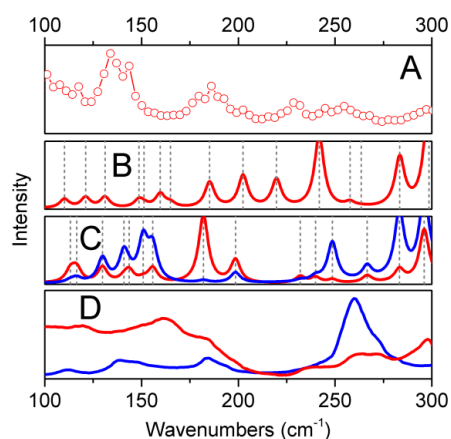


Fig. S6. Panel A: Fourier transform spectrum of the residual oscillations from the time dependent response in the spectral ranges of the excited state responses at 1550 cm^{-1} , as shown in Fig. 6 in the main text and discussed there. Panel B: grey dashed lines indicate calculated resonances of low frequency normal modes of *cis* indigo carmine model molecule in the first electronic excited state; red line represents the Infrared spectrum. Panel C: grey dashed lines indicate calculated resonances of low frequency normal modes of *cis* indigo carmine model molecule in the electronic ground state; red and blue lines show normalized Infrared and Raman spectra. Panel D: FTIR spectrum of solid indigo carmine (red line), and resonant Raman spectrum (blue line) of indigo carmine solution in deuterated DMSO detected using excitation at 532 nm.

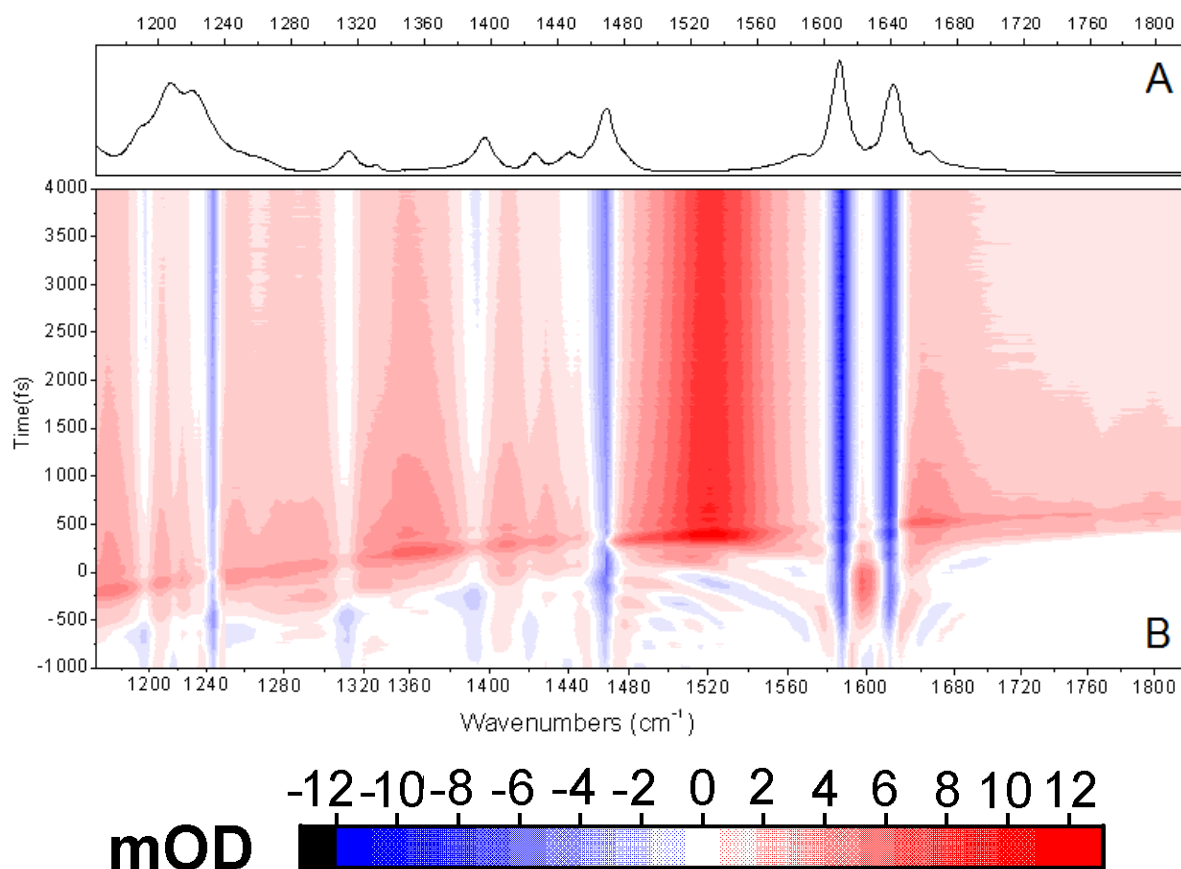


Fig. S7. Panel A: FTIR for solution of indigo carmine in deuterated DMSO. Panel B: time resolved differential infrared response of indigo carmine in deuterated DMSO after excitation at 630 nm.

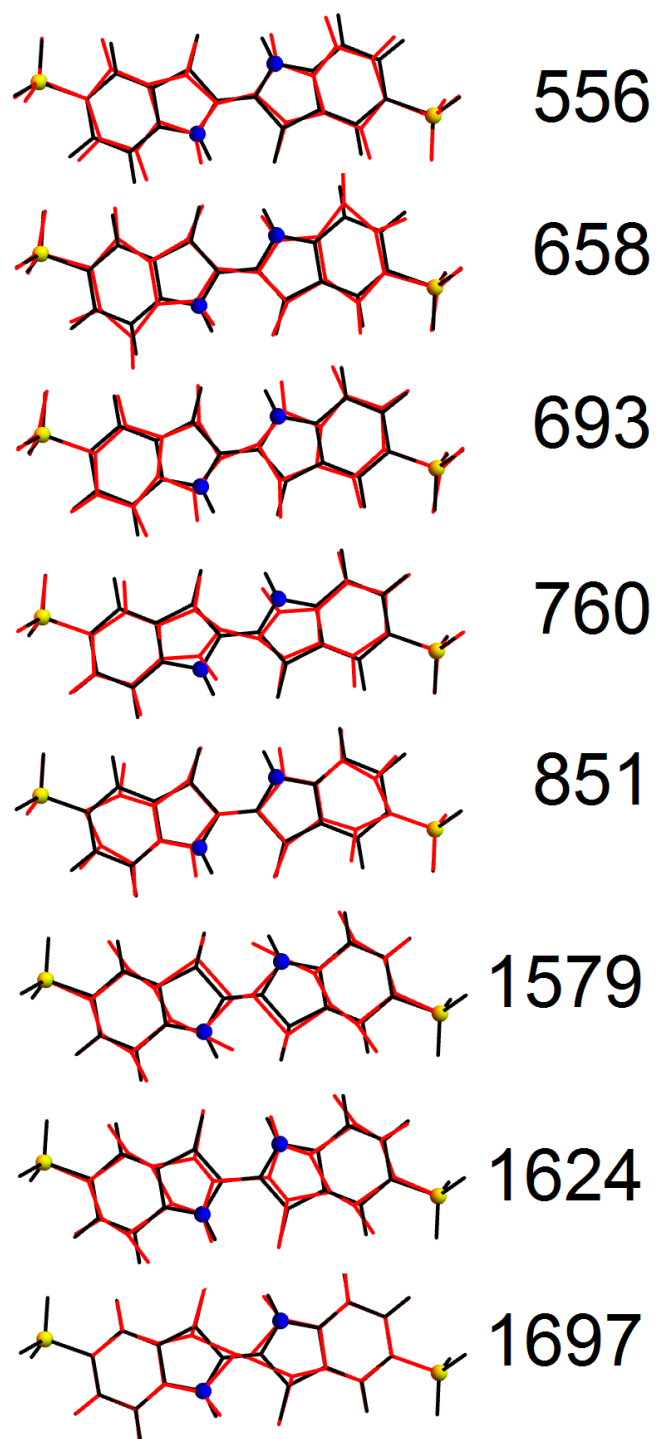


Fig. S8. Enlarged views for the graphical representations of the main Raman active normal modes at the anticipated frequencies (scaling factor is 0.97) of *trans* indigo carmine in the electronic ground state by DFT, as shown in Fig. 3 in the main text.

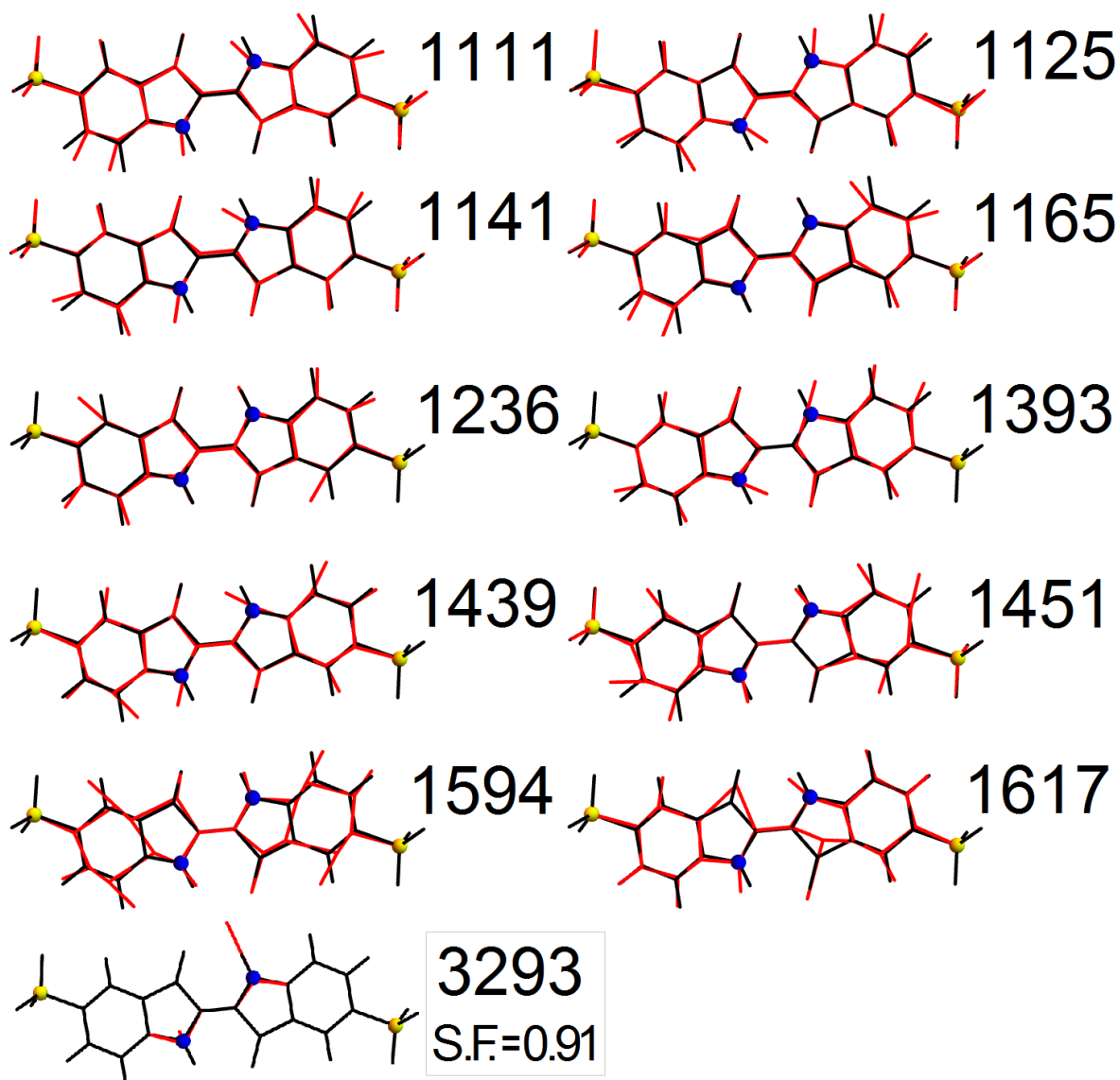


Fig. S9. Enlarged views for the graphical representations of the main IR active normal modes at the anticipated frequencies (scaling factor is 0.97) of *trans* indigo carmine in the electronic ground state by DFT and using PCM, as shown in Fig. 4B in the main text.

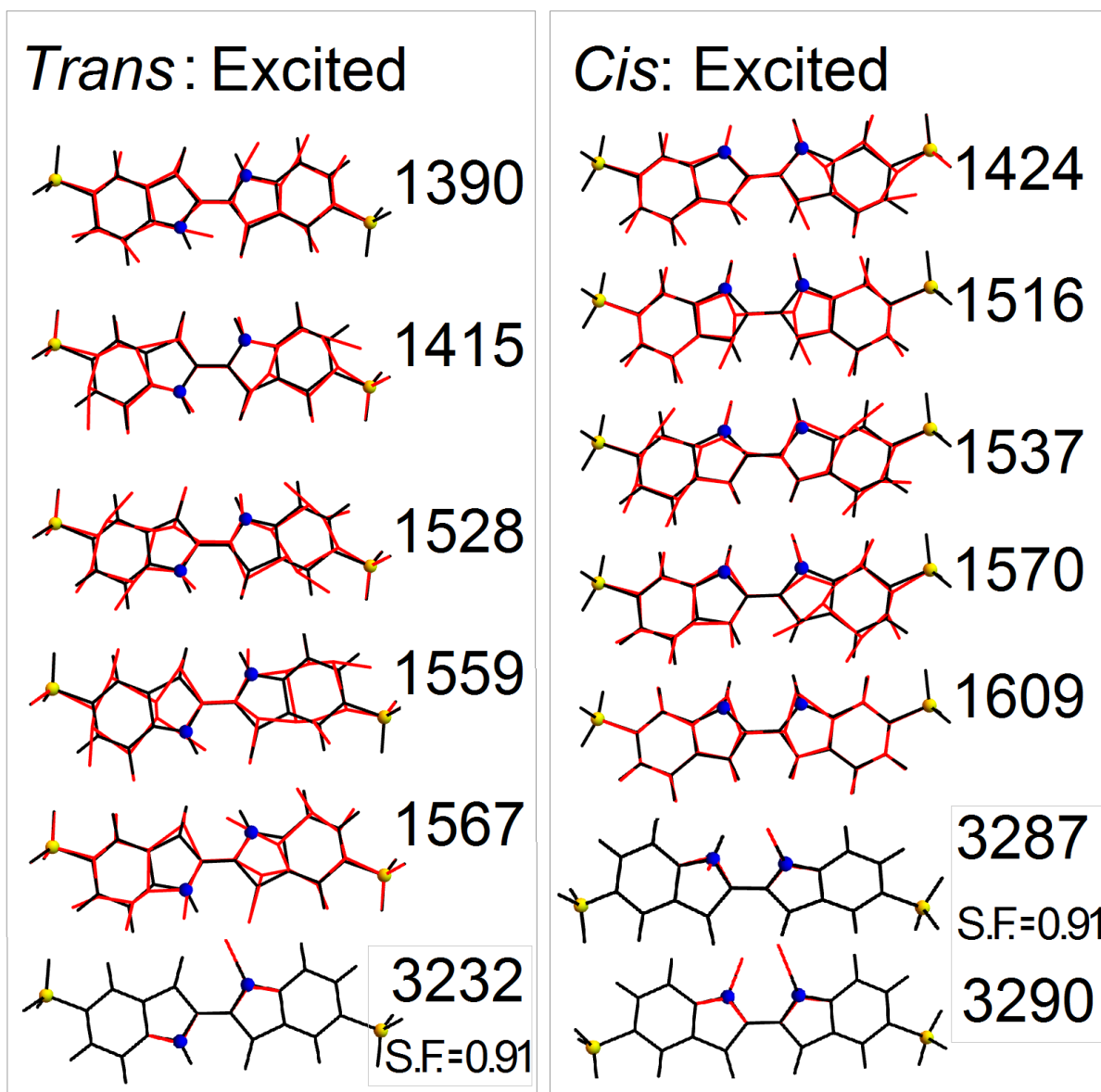


Fig. S10. Enlarged views for the graphical representations of the main IR active normal modes at the anticipated frequencies (scaling factor is 0.97) of *trans* and *cis* indigo carmine in the electronic excited state by TD-DFT and using PCM, as shown in Fig. 4C and 4D in the main text.

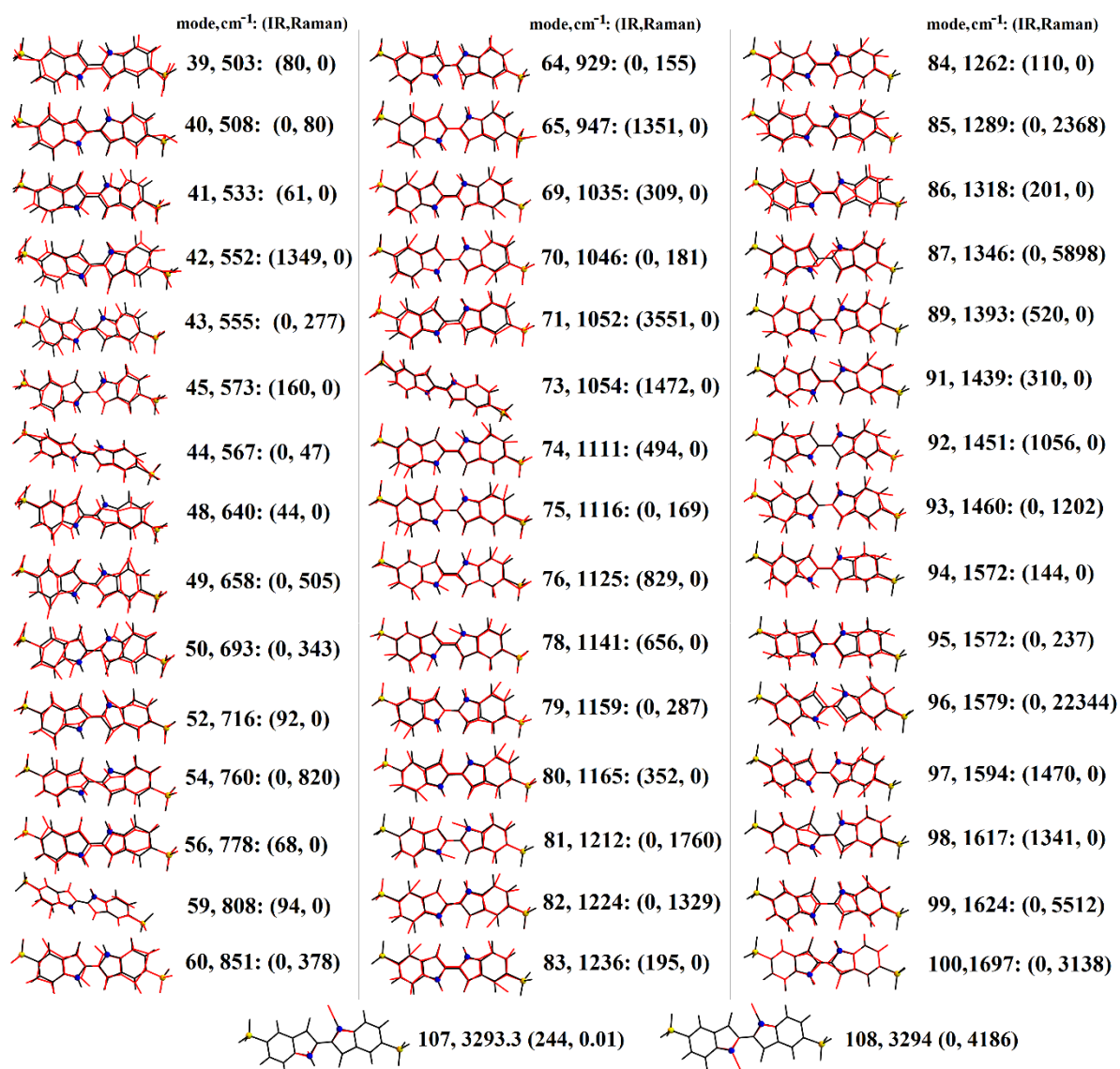


Fig. S11. Graphical representations of normal modes with relevant optical activities of *trans* indigo carmine in the electronic ground state in the spectral range between 500 and 1700 cm⁻¹ by DFT using PCM. For each case we show the number of the mode, its frequency and, in brackets, IR and Raman intensities. Scaling factor for all modes but 107 and 108 is 0.97. Scaling factor for the modes 107 and 108 is 0.91.

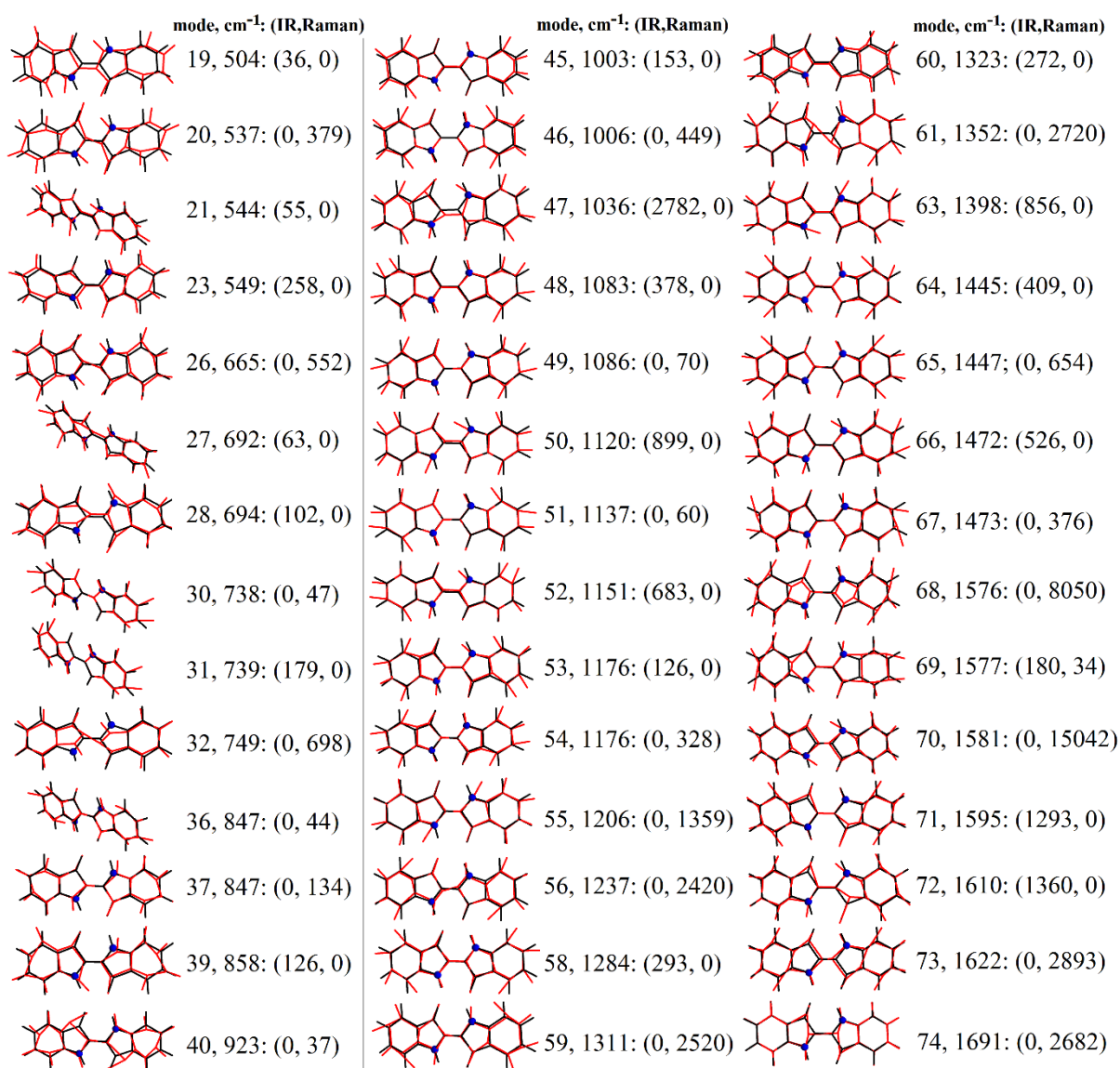


Fig. S12. Graphical representations of normal modes with relevant optical activities of *trans* indigo in the electronic ground state in the spectral range between 500 and 1700 cm⁻¹ by DFT using PCM. For each case we show the number of the mode, its frequency (scaling factor is 0.97) and, in brackets, IR and Raman intensities.

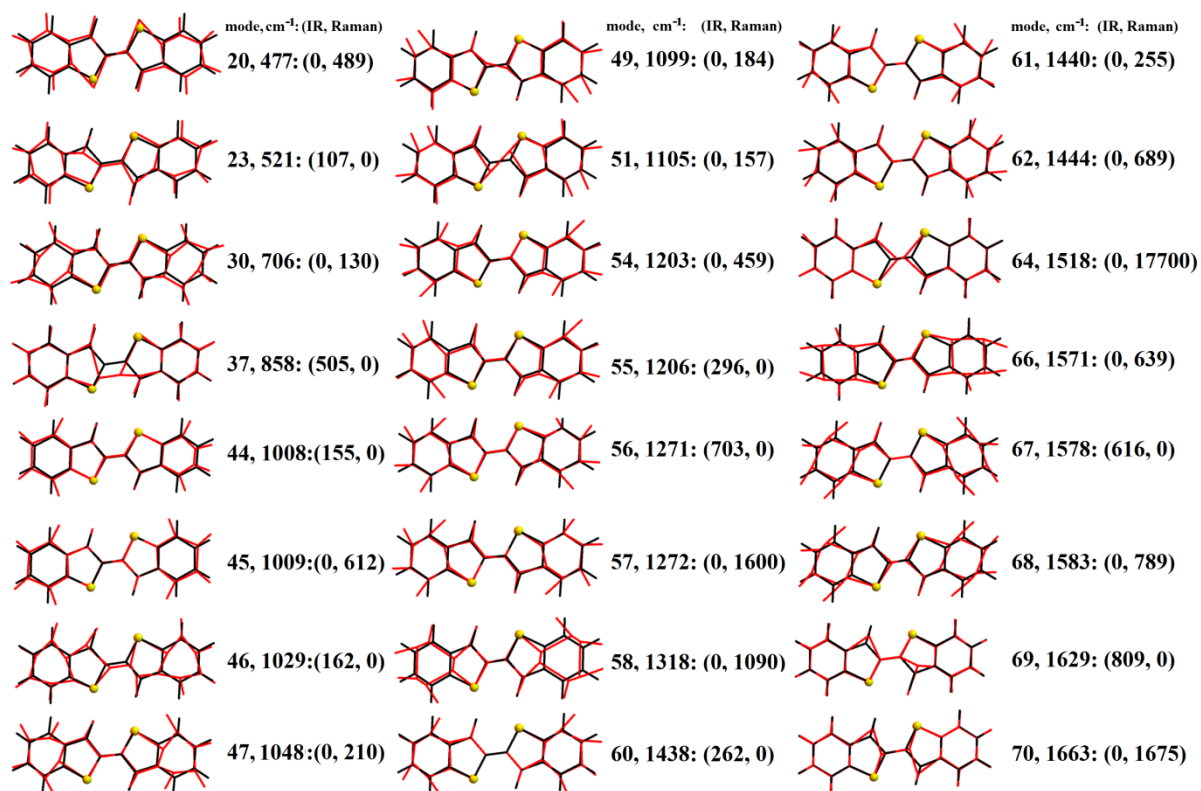


Fig. S13. Graphical representations of normal modes with relevant optical activities of *trans* thioindigo in the electronic ground state in the spectral range between 500 and 1700 cm⁻¹ by DFT using PCM. For each case we show the number of the mode, its frequency (scaling factor is 0.97) and, in brackets, IR and Raman intensities.